A Study on Fatigue Damage Modeling Using Neural Networks

Dong-Woo Lee
*Department of Mechanical Engineering, Dong-A University,
Busan 604-714, Korea*

Soon-Hyeok Hong
*Cooperative Laboratory Center, Pukyong National University,
Busan 608-739, Korea*

Seok-Swoo Cho*
*Department of Vehicle Engineering, Samcheok National University,
Samcheok 245-711, Korea*

Won-Sik Joo
*Department of Mechanical Engineering, Dong-A University,
Busan 604-714, Korea*

Fatigue crack growth and life have been estimated based on established empirical equations. In this paper, an alternative method using artificial neural network (ANN)-based model developed to predict fatigue damages simultaneously. To learn and generalize the ANN, fatigue crack growth rate and life data were built up using in-plane bending fatigue test results. Single fracture mechanical parameter or nondestructive parameter can't predict fatigue damage accurately but multiple fracture mechanical parameters or nondestructive parameters can. Existing fatigue damage modeling used this merit but limited real-time damage monitoring. Therefore, this study shows fatigue damage model using backpropagation neural networks on the basis of X-ray half breadth ratio B/B_o, fractal dimension D_f and fracture mechanical parameters can estimate fatigue crack growth rate da/dN and cycle ratio N/N_f at the same time within engineering limit error (5%).

1. Introduction

Mechanical failures have caused many injuries and much financial loss. No exact percentage is available, but many books and articles have suggested that between 50 and 90 percent of all mechanical failures are fatigue failure. To be effective in averting fatigue failure, it is essential for a

---

* Corresponding Author,
E-mail : sscho394@samcheok.ac.kr
TEL : +82-33-570-6394; **FAX :** +82-33-570-6390
Department of Vehicle Engineering, Samcheok National University, Samcheok 245-711, Korea. (Manuscript **Received** November 29, 2004; **Revised** December 15, 2004)

designer to have a good working knowledge of analytical and empirical techniques of predicting fatigue failure so that fatigue failure during the prescribed design life may be prevented.

Fatigue crack growth rate can be expressed in terms of stress intensity factor range ΔK or effective stress intensity factor Δ_{eff} on the basis of crack closure concept. the former and latter were suggested by Paris and Elber, respectively. As correlating parameters for the fatigue crack growth rate in the plastic-elastic region, J-integral range ΔJ is proposed but breaks a definition of J-integral because it doesn't include unloading process. The fatigue life was represented as a function of plastic strain range $\Delta \varepsilon_p$ at low-cycle fatigue and

stress amplitude $\Delta\sigma$ at high-cycle fatigue.

Fatigue resistance of material is estimated by fracture mechanical parameters, but there is a sharp difference between fatigue crack growth rate and fatigue life due to various loads and materials, and environmental factors. Especially, in case that there is a short crack or no notch on surface, the existing estimation method of fatigue fracture behavior can't be adapted because fatigue life or fatigue crack growth rate is influenced by microstructure properties of material. Therefore, fatigue damage can't be estimated by only single mechanical parameter. A considerable error shall occur between actual and estimated fatigue damage and be reduced by using some mechanical parameters simultaneously.

Joo and Cho (1996a) investigated the fatigue crack growth modeling by ANN. Its input units and output units consisted of elastic-plastic fracture mechanical parameters and fatigue crack growth rate respectively. The scatter band estimated from the existing empirical equation showed factors of 2 on fatigue crack growth rate. But the fatigue crack growth modeling by neural network prepared crack growth data with two and three point representation schemes and predicted the crack growth rate for unlearned test condition with a mean error of 5%.

Okuda and others (1996) developed neural network-based model representing the stress-strain behavior of high temperature material. They used plastic strains and their gradients as the units of input and output layers and predicted the stress-strain diagram for unlearned data with an error of less than 3%.

Wu and others (1993) showed that with a neural network based material modeling methodology, the stress-strain behavior of a material was captured within the distributed weight structure of a multilayer feed forward neural network learned directly on the stress strain data obtained from experiments. The general applicability of the approach was illustrated in the construction of a composite material model for reinforced concrete in a biaxial stress state by learning stress-strain results on behaviors of reinforced concrete panels tested in both pure shear and combined shear

with normal stress. However, above-mentioned modeling methods couldn't estimate the material behavior at real-time due to the limit of representation schemes.

In this study, a new and alternative approach is developed known as the ANN for the synthetical estimation of fatigue damage. It estimates crack growth rate da/dN and cycle ratio N/N_f using X-ray half value breadth ratio B/B_0, fractal dimension D_f and fracture mechanical parameters, simultaneously.

2. Theoretical Background of ANN

2.1 Structure and learning algorithm of ANN

Figure 1 shows the multilayer neural networks which consist of input units, hidden units and output units. A neuron is denoted by the hollow circle in the figure and has a high-dimensional input vector and one single output vector which is a non-linear function of the input vector and a weight vector. This weight vector is adjusted in a learning phase by using large sets of examples and a learning rule. The learning rule adapts the weight of all neurons in neural networks to learn an underlying relation in the learning examples. The central idea of a neural network is that all the weights can be adjusted so that the networks exhibits some desired or interesting behavior. The learning algorithms used in this study is the backpropagation algorithms, which propagates
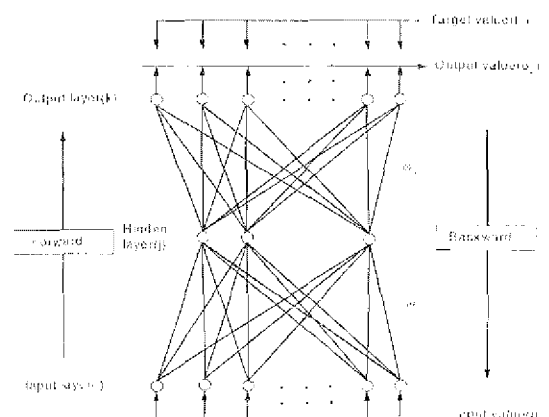

Fig. 1   Block of backpropagation neural networks

the output error, back to each weight in the networks.

When a pattern between input layer data and output layer data is recognized and stored within connection weight matrix, a learning of ANN is completed. A new output data is obtained, when unlearned input layer data is substituted into a connection weight matrix. If the output layer data is converged to target value of mean error, the ANN will have a generalizing capacity.

Error function E_p between target value and actual output value of input pattern P is as follows :

$$E_p = 1/2 \sum (t_{pj} - o_{pj})^2 \qquad (1)$$

E_p : (Error for data pattern P)^2
t_{pj} : Target value of j-th unit at output layer
o_{pj} : Output value of j-th unit at output layer

Eq. (2) is obtained by steepest descent method and is used to update the connection weight between units.

$$\Delta_p \omega_{ji}(n+1) = \eta \delta_{pj} + \alpha \Delta_p \omega_{ji}(n) \qquad (2)$$

n : Learning epochs
η : Learning rate
α : Momentum rate
Δ_p : Variation of connection weight
δ_{pj} : Error signal of j-th unit at step n

A Learning and generalizing capacity of ANN is estimated by the difference between output values and target values of ANN. It is called by estimated mean error (error). Its definition is as follows :

$$\phi = \frac{1}{r} \sum_{p=1}^{r} \frac{|\phi_{neuro}(p) - \phi(p)|}{|\phi(p)|} \qquad (3)$$

where, $\phi(p)$ is a target value for input layer unit, r is number of learning data used in learning and generalization and $\phi_{neuro}(p)$ is output value of ANN for input layer unit. It is assumed that when the estimated mean error is converged within 0.05, ANN has a very good accuracy of modeling.

3. Estimation of Fatigue Damage Using Destructive and Non-Destructive Parameters

The specimens used in this study were a flat plate type with a curvature radius of 39 mm. Notch specimen had a micro-hole defect with a diameter of 50 μm and a depth of 10 μm at its center. Fatigue life of notch specimen with micro-hole defect was 2530~4780 cycles and fatigue life of unnotched specimen was 2530~4780 cycles so that the change of fatigue life due to micro-hole defect was only a little. The micro-hole defect which was less than critical crack size don't had little influence on fatigue strength. Thus, micro-hole defect specimen was used for this study because main crack growed at micro-hole defect and was measured with ease.

Also, fatigue test was controlled to be stress ratio -1 using in-plane bending fatigue tester (Mori testing machine co., model 5171) (Joo et al., 1998a). Crack growth rate da/dN, cycle ratio N/N_f and fatigue damage estimation parameters were based on the test result of Al 2024-T3 alloy examined in previous work by the authors (Joo et al., 1998a ; Kim, 1998 ; Jang et al., 1999). The fatigue testing was stopped at interval of same cycle ratio regularly and fatigue damage parameters were estimated at the time.

Table 1 shows tensile test results for 2024-T3 aluminum alloy.

3.1 Estimation of crack growth rate da/dN by $(\Delta \sigma / \sigma_{ys})^m a^n$

It is very difficult to measure the shape of surface crack for calculation of stress intensity factor. The growth rate of surface crack couldn't be estimated by stress intensity factor (Tanaka, 1982). Crack growth rate was correlated well

Table 1 Mechanical properties of 2024-T3 alloy

Material	Yield strength σ_{ys} (MPa)	Tensile strength σ_{ts} (MPa)	Elongation ε (%)	Young's moudlus E (GPa)
2024-T3	380	507	21.6	77.02
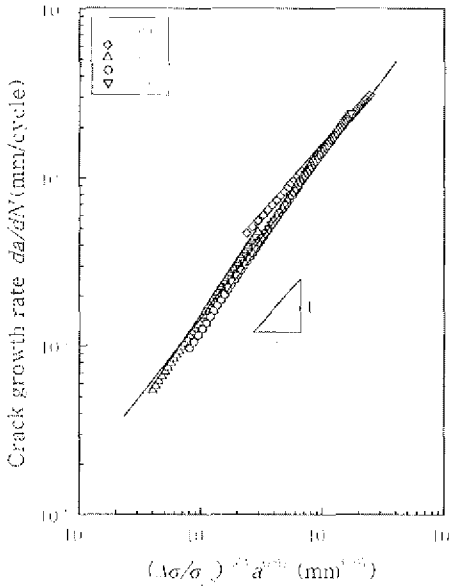
Fig. 2 Relation between crack growth rate da/dN and $(\Delta\sigma/\sigma_{ys})^{4.64}a^{0.67}$

Fig. 3 Relation between half-value breath ratio B/B_0 and cycle ration N/N_f

with $(\Delta\sigma/\sigma_{ys})$ and crack length a. All the data obtained under each test condition form wide scatter band of either $da/dN - (\Delta\sigma/\sigma_{ys})$ relationship or $da/dN - a$ relationship. The expressions of fatigue crack growth behavior are as follows.

$$da/dN = \Lambda (\Delta\sigma/\sigma_{ys})^m \qquad (4)$$

$$da/dN = B(a)^n \qquad (5)$$

Exponent m shows an average gradient at $da/dN - (\Delta\sigma/\sigma_{ys})$ diagram and is 4.64 in case of the material. Exponent n is an average gradient at $da/dN - a$ diagram and 0.67 in case of the material. Fig. 2 presents all the results on crack growth rate as function of fracture mechanical parameter $(\Delta\sigma/\sigma_{ys})^{4.64}a^{0.67}$ (Hironobu Nishitani, 1985). All the data obtained under each test condition fell within narrow scatter band. If we assume the relationship of one type of form :

$$da/dN = (\Delta\sigma/\sigma_{ys})^{4.64}a^{0.67}$$

3.2 Estimation of cycle ratio N/N_f by X-ray half-value breadth ratio B/B_0

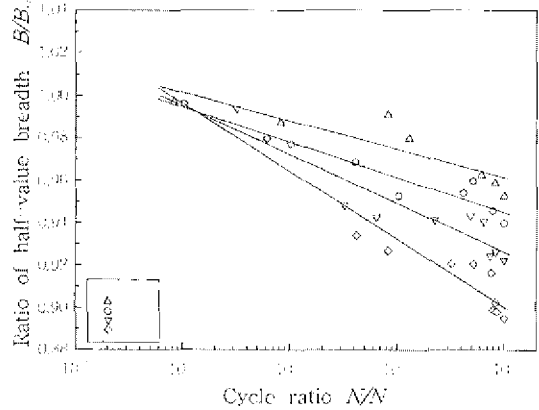In order to analyze the X-ray half-value breadth, X-ray diffractometer that adapts the

characteristic X-ray of Cr-K$_a$ was used. When measuring the Half-value breadth, parallel beam optics was used and the X-ray incident angle was fixed to $0°$. X-ray diffraction strength curve is obtained at each cycle ratio N/N_f. Half-value breadth was the diagram breadth at $1/2$ of maximum strength I_{max} in X-ray diffraction strength curve. Therefore, half-value breadth ratio B/B_0 means a ratio of half-value breadth B at any cycle ratio over half-value breadth B_0 at initial cycle ratio (Park et al., 1998).

Figure 3 shows the relationship between X-ray half-value breadth ratio B/B_0 and cycle ratio N/N_f in Al 2024-T3 alloy (Joo et al., 1998a). At the beginning of fatigue life, X-ray half-value breadth ratio B/B_0 decreased rapidly at initial stage of fatigue life. So the data is excluded in linear regressed data and is omitted in Fig. 3. Except for initial stage of fatigue life, X-ray half value breadth ratio B/B_0 decreased slowly as cycle ratio N/N_f increased but at the last stage of fatigue life, it decreased rapidly like initial stage of fatigue life. Also the straight line in Fig. 3 is linearly regressed with least square method. The gradient of line varies according to the stress amplitudes, and the more increased the stress amplitude, the more increased the gradient. Fig. 3 shows dependence of stress amplitude $\Delta\sigma$ for X-ray half-value breadth ratio B/B_0 at observed cycle ratio N/N_f. The more increased stress amplitude, the more increased X-ray half-value

breadth ratio B/B_0. This result is because initiation and growth of short crack by formation of cyclic slip band is sensitive to stress amplitude and number of cycle.

3.3 Estimation of cycle ratio N/N_f by Fractal dimension D_f

Fatigue crack shape has a irregular form, not primary straight line. As applied load gets larger, crack shape gets more complicated. This section will apply above crack characteristic to fatigue life estimation.

Mandelbert (1983) suggested fractal dimension D_f, the ratio of logarithmic number of subpart for logarithmic scale factor in order to represent complexity of curve shape. In this study, the box-counting method is applied to determine the fractal dimension of crack shape. It was measured at each cycle ratio.

Figure 4 shows fractal dimension D_f of fatigue crack shape at each cycle ratio N/N_f. The fractal dimension D_f increases with nearly linearly with the increase of cycle ratio N/N_f. The more increased stress amplitude the more increased the whole fractal dimension D_f. However, in case of stress amplitude $\Delta\sigma = 262$ MPa, the gradient of regression line is very steep because fractal dimension D_f is the lowest at initial fatigue life and the highest at final fatigue life stage.

This result shows that fatigue damage can't be estimated by only fractal dimension D_f because

fractal dimension D_f increases in accordance with cycle ratio N/N_f but it depends on initial crack shape and material structure strongly.

4. Result and Examination of Fatigue Damage Modeling

4.1 Fatigue damage modeling parameters and data pattern

For fatigue damage analysis, there were the test conditions that was used as learning data sets (respectively, $\Delta\sigma = 225$ MPa, 262 Mpa, 330 MPa). After the learning, generalization is attempted at, using prediction data set ($\Delta\sigma = 303$ MPa), which falls inside the learning domain (interpolation).

Figure 5 represents the basic architecture of ANN for fatigue damage modeling.

Number of input units : there were five units in the basic structure. These five input units corresponded to real measurable parameters (stress amplitude $\Delta\sigma$, X-ray half-value breadth ratio B/B_0, fractal dimension D_f, crack length a and fracture mechanical parameter $(\Delta\sigma/\sigma_{ys})^{4.64} a^{0.67}$.

Number of output units : There are altogether two typical fatigue damage parameters. Crack growth rate and cycle ratio corresponded to the two output units.

ANN parameters arrived at optimum values which gives minimum error, after the successful phase are given in Table 3. Before arriving at this optimum, the range of values were shown in Table 2. The table represents initial conditions of
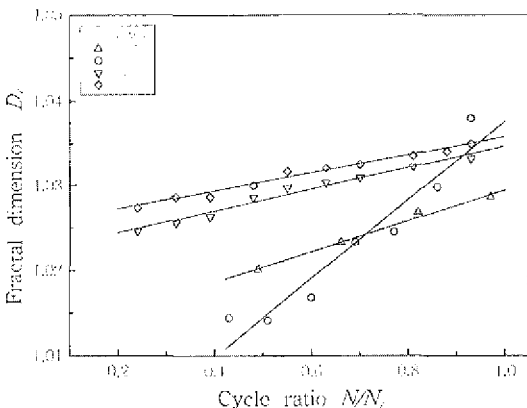

Fig. 4 Relation between ratio of fractal dimension D_f and cycle ration N/N_f
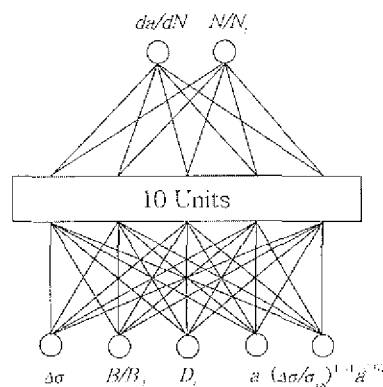

Fig. 5 Architecture of ANN in fatigue damage modeling

ANN for fatigue damage modeling.

In order to optimize ANN parameters, one parameter is changed constantly and other parameters are fixed in the condition of Table 2. The ANN was learned according to varying conditions. When the learning error is minimized, it is said that the ANN parameters is optimized.

Table 3 represents the ANN parameters which is determined by above-mentioned method (fixed rate method). Also, Table 4 shows rate transformation method, which changes each rate in accordance with number of learning in order to recover defect of the fixed rate method that learning and momentum rates are fixed regardless of number of learning. Learning and momentum rates in Table 3 have the same as case 5 in Table 4.

4.2 Estimation of fatigue damage by fatigue damage modeling

4.2.1 Estimation of fatigue damage by optimization of initial learning conditions

The symbols indicating the learning in Figs. 6, 8 and 10 are the same as them in Figs. 2, 3, and 4 and shows learning result by ANN. Solid line is regressed by experiment data used for learning. Also solid line of Figs. 7, 9 and 11 related to generalization is the same as above figures for learning but dotted line shows the estimation of fatigue crack growth rate and cycle ratio using ANN.

Figures. 6 and 7 show the learning and generalization results of ANN according to learning condi-

Table 2　Initial conditions for learning of ANN

No. of Hidden layer	No. of hidden units	Learning rate	Momentum rate	No. of data	No. of epochs
1	10	0.1	0.9	51	100000

Table 3　Optimal conditions and estimated mean error or learning of ANN

Parameter		No. of Hidden layer	No. of Hidden units	Learning rate	Momentum Rate	No. of data	No. of epochs
Optimal conditions		1	6	0.9	0.9	51	2000000
Estimated mean error	da/dn	0.0738	0.0243	0.06523	0.13015	0.0243	0.0140
	N/N_f	0.01101	0.0100	0.02502	0.03908	0.0100	0.0049

Table 4　Change of momentum and learning rate with number of epochs

Case Rate		Epochs 20000	40000	60000	80000	100000
Case 1	Learning rate	0.9	0.7	0.5	0.3	0.1
	Momentum rate	0.9	0.7	0.5	0.3	0.1
Case 2	Learning rate	0.1	0.3	0.5	0.7	0.9
	Momentum rate	0.1	0.3	0.5	0.7	0.9
Case 3	Learning rate	0.9	0.7	0.5	0.3	0.1
	Momentum rate	0.1	0.3	0.5	0.7	0.9
Case 4	Learning rate	0.1	0.3	0.5	0.7	0.9
	Momentum rate	0.9	0.7	0.5	0.3	0.1
Case 5	Learning rate	0.9	0.9	0.9	0.9	0.9
	Momentum rate	0.9	0.9	0.9	0.9	0.9

tions of Table 3. The learning errors of ANN are within engineering limit error 0.05 because they are 0.014 in case of crack growth rate da/dN and 0.0049 in case of cycle ratio N/N_f. However, The generalization errors of ANN exceed an engineering limit error 0.05 because they are 0.151 in case of crack growth rate da/dN and 0.2785 in case of cycle ratio N/N_f. It is observed that the predictive capability of ANN is very poor. It is well known in ANN approaches that trans-

formation or combinations of parameters may describe the problem more effectively than the individual parameters themselves. Combination of parameters for ANN was selected by previous papers (Kim, 1998). Even though the ANN is learned much enough, the data ranges of X-ray half-value breadth ratio B/B_0 and fractal dimension D_f are 0.93376~1 and 0.97182~1, respectively. Hence an attempt should be made to transform certain parameters. We propose a data trans-
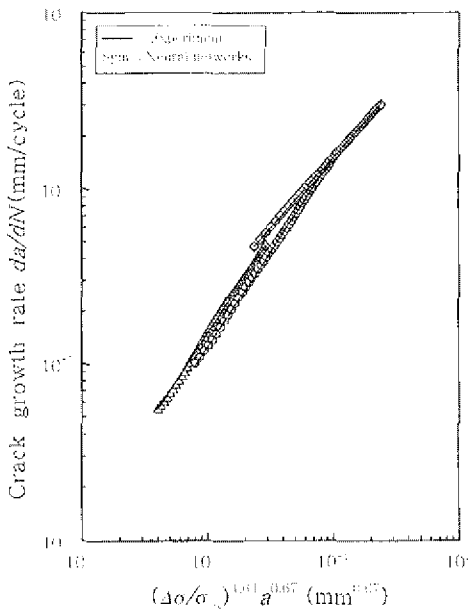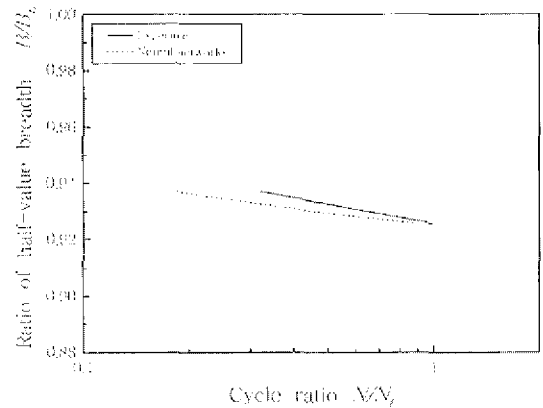

(a) Unit da/dN at output layer
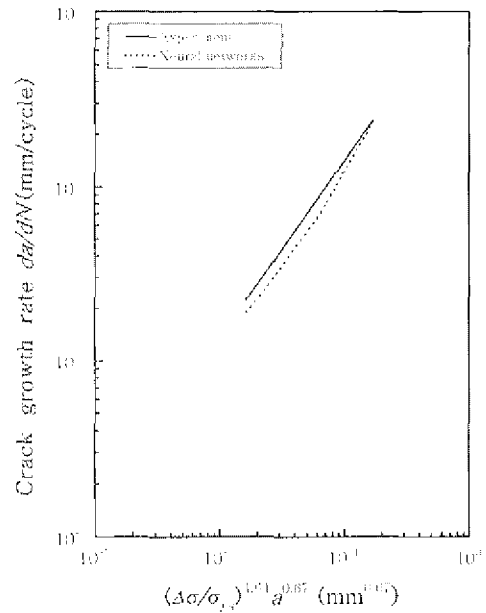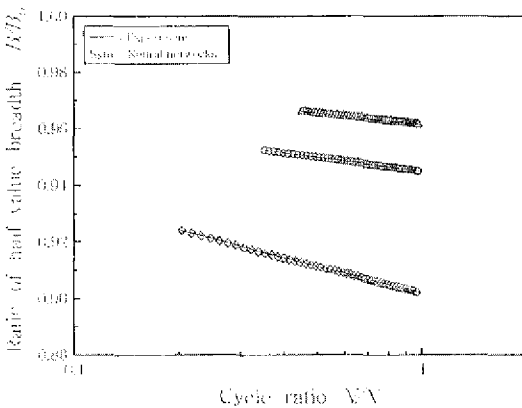
(b) Unit N/N_f at output layer

Fig. 6 Crack growth rate da/dN and cycle ratio N/N_f learned by ANN with initial learning conditions

(a) Unit da/dN at output layer

(b) Unit N/N_f at output layer

Fig. 7 Crack growth rate da/dN and cycle ratio N/N_f predicted by ANN with initial learning conditions

Table 5 Estimated mean error of learning and generalization of ANN with data transformation method

Error	Case	Case 1	Case 2	Case 3	Case 4	Case 5
Estimated mean Error of learning	da/dn	0.0513	0.0111	0.0172	0.0168	0.0129
	N/N_f	0.0098	0.0030	0.0039	0.0043	0.0047
Estimated mean Error of generalization	da/dn	0.0828	0.0732	0.0932	0.0488	0.0692
	N/N_f	0.0541	0.2559	0.2265	0.0321	0.3053

formation method which controls data artificially in order to improve the poor recognition capability of learning pattern in next section 4.2.2.

4.2.2 Estimation of fatigue damage by data transformation method

Fatigue damage is sensitive to the variation of X-ray half-value breadth ratio B/B_0 and fractal dimension D_f. These parameters need to transform the data range using following equations.

$$(B/B_0)' = 10(N/N_f) + B/B_0 \qquad (6)$$

$$D_f' = 10(N/N_f) + D_f \qquad (7)$$

$(B/B_0)'$: Rescaled value of B/B_0
D_f' : Rescaled value of D_f

Table 5 shows the learning and the generalization results of ANN by means of data transformation method. In both of section 4.2.1 and case 5 of Table 5 the modeling is reasonably accurate except for the generalization result of cycle ratio N/N_f. The learning and generalization results of the ANN after transformation of parameter are superior to them before transformation of parameters. Especially, the generalization error of crack growth rate da/dN after transformation of parameters is reduced at 1/2 and then it is shown that the learning and generalization results of ANN are very dependent on the data range.

Figures 8 and 9 show the learning and generalization results for case 5 of Table 5. Crack growth rate da/dN and cycle ratio N/N_f learnings are produced at engineering limit error 0.05 level but crack growth rate da/dN and cycle ratio N/N_f generalizations aren't produced. Especially, the dispersion the dotted line about the solid line in Fig. 9(b) is a result of inaccuracies in the ANN.

These inaccuracies are due to the lack of a deterministic relationship between the inputs and outputs. Cycle ratio N/N_f has a great error between the beginning and middle stage of fatigue life. Also, the learning error is the lowest in case 2 but the generalization error is the highest in case 2 and is the lowest in case 4 in which there are no considerable character in learning process. This result indicates that ANN has an enough error restoration capacity for unlearned data in spite of inaccurate mapping of data pattern.

4.2.3 Estimation of fatigue damage by rate transformation method

Figures 10 and 11 show the learning and generation results of ANN on the basis of learning and momentum rates of case 4. The learning error is higher than that of other rate selection methods but the generalization error is the lowest (0.0488 in case of crack growth rate da/dN and 0.0321 in case of cycle ratio N/N_f).

4.2.4 Estimation of cycle ratio N/N_f by crack growth equation and ANN

The difference between parameters for optimization of ANN and parameters by rate selection method is due to the distribution characteristics of the connection weights between the input and output units which recognize the data pattern of ANN.

$$\frac{da}{dN} = \frac{1}{C}[(\Delta\sigma/\Delta_{ys})^m a^n]$$
$$= 1.43 \times 10^{-3}[(\Delta\sigma/\sigma_{ys})^{4.64} a^{0.67}] \qquad (8)$$

where $C(1/1.43 \times 10^{-3})$, $m(4.64)$, and $n(0.67)$ are material constants that were determined experimentally. Please refer to previous papers (Jang et al., 1999). The cycles required for crack

growth may be calculated by solving this equation for dN and integrating both sides

$$\int_0^{N_f} dN = \int_{a_0}^{a_f} C \left(\frac{\sigma_{ys}}{\Delta\sigma} \right)^m \left(\frac{1}{a} \right)^n da$$

$$N_f = C \left(\frac{\sigma_{ys}}{\Delta\sigma} \right)^m \int_{a_0}^{a_f} \left(\frac{1}{a} \right)^n da \qquad (9)$$

$$= C \left(\frac{\sigma_{ys}}{\Delta\sigma} \right)^m \left[\ln \frac{a_f}{a_o} \right]^n$$

Initial crack is often assumed to exist at a certain location in the structure. In eq. (9), initial crack length a_o is assumed to be regarded as 0.05 mm. Final crack size a_f is the crack length corresponded to $N/N_f = 0.99$ from $a-N/N_f$ relationship. In case of $\Delta\sigma = 303$ MPa, the number of cycle to fracture N_f is 29078 by eq. (9) but measured number of cycle to fracture N_f is 43400. So, the measured and predicted data show 33% error. This is an indication that the crack growth equation has no regard for crack initiation cycles N_i.
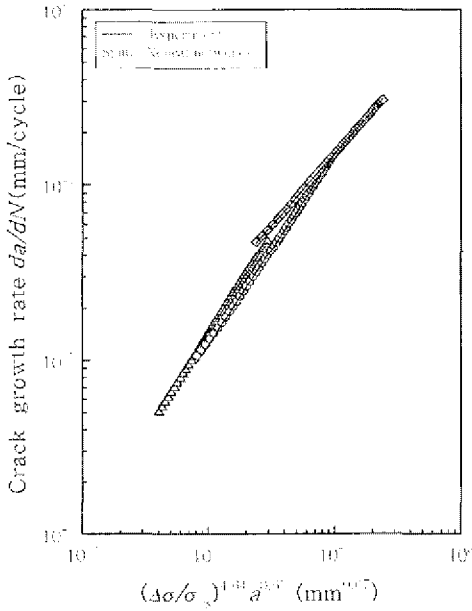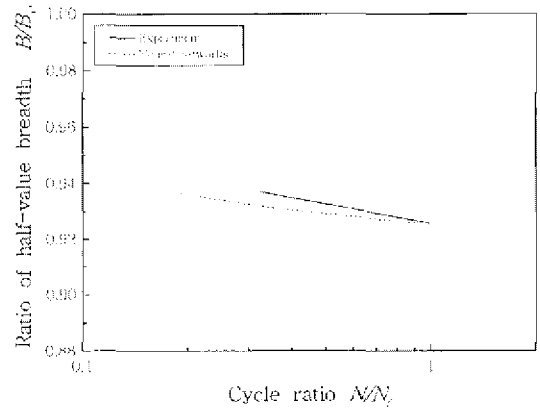

(a) Unit da/dN at output layer
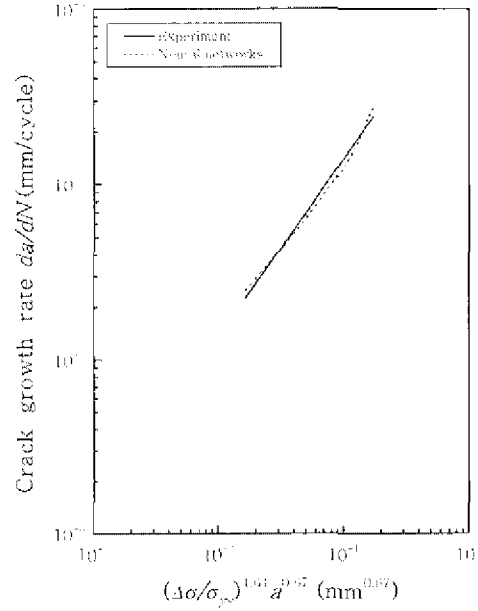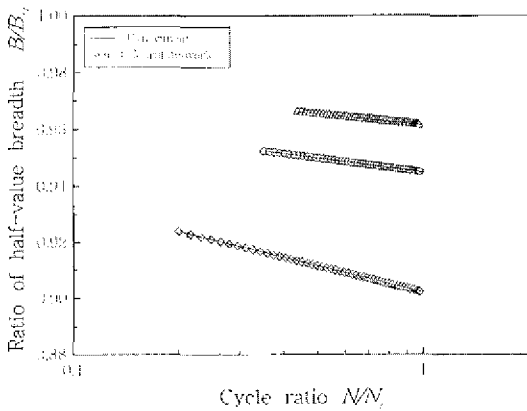
(b) Unit N/N_f at output layer

Fig. 8   Crack growth rate da/dN and cycle ratio N/N_f learned by ANN with data transformation

(a) Unit da/dN at output layer
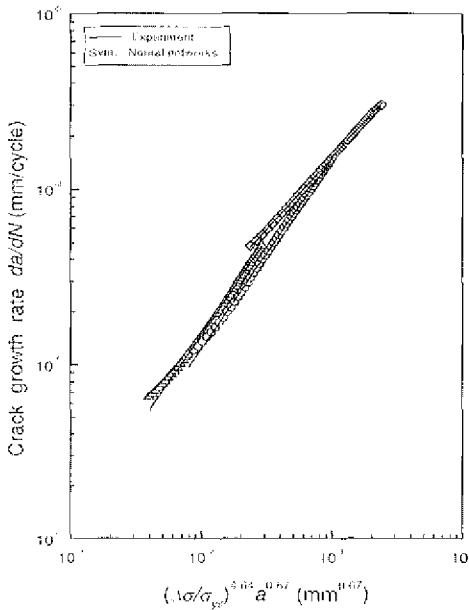

(b) Unit N/N_f at output layer

Fig. 9   Crack growth rate da/dN and cycle ratio N/N_f predicted by ANN with data transformation

Above approach is not useful in Al 2024–T3 alloy (the material used in this study), whose crack initiation cycles take up most fatigue life.

In Fig. 12, the predicted cycles ratio was compared with those obtained from the experiment. One is predicted by eq. (8) and another is predicted by ANN. For measured cycle ratio $N/N_f = 0.99$, the cycle ratio N/N_f estimated by crack growth equation is 0.67 but the cycle ratio N/N_f predicted by ANN is 0.963. It can be

clearly understood that the cycle ratio obtained from the learned ANN shows good agreement with that from the learned ANN compared with that obtained from the crack growth equation. The ANN approximates cycle ratio better than the crack growth equation. This result is an indication that the number of cycle to crack initiation N_i is recognized by various parameters during learning process.
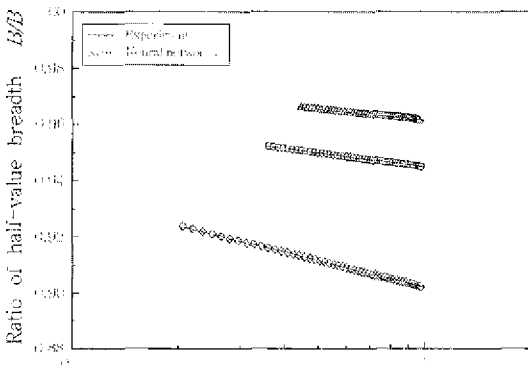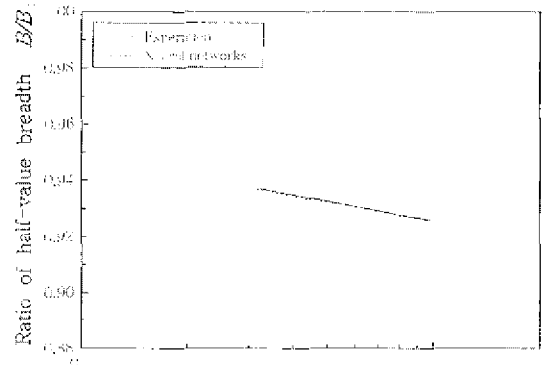
Therefore, the results prove that the ANN

(a) Unit da/dN at output layer
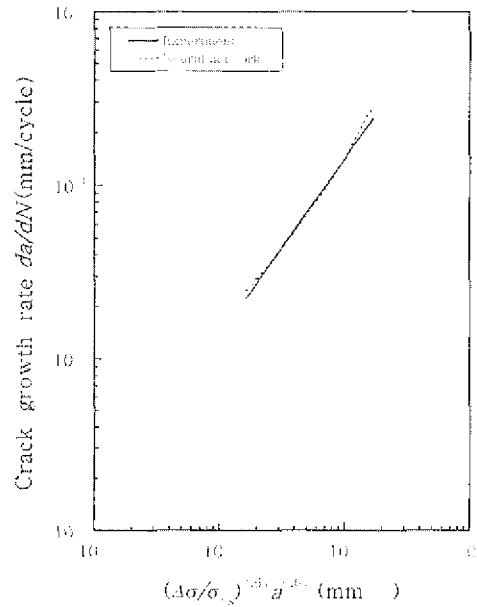
(b) Unit N/N_f at output layer

Fig. 10 Crack growth rate da/dN and cycle ratio N/N_f learned by ANN with floating rate method

(a) Unit da/dN at output layer

(b) Unit N/N_f at output layer

Fig. 11 Crack growth rate da/dN and cycle ratio N/N_f predicted by ANN with floating rate method
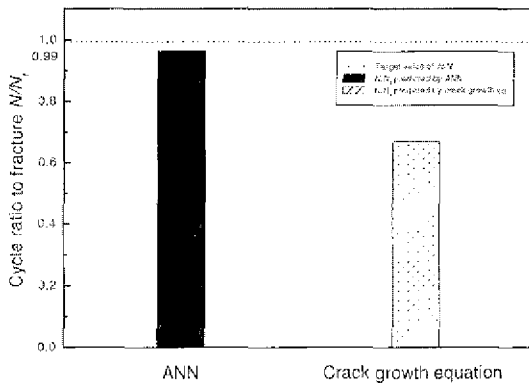
Fig. 12 Prediction of cycle ratio to fracture N/N_f by ANN and crack growth equation

which learns failure & fracture process can be used to replace the crack growth equation to estimate the cycle ratio on unlearned data points with higher accuracy and reliability.

5. Conclusion

The main objective of this study was to introduce a new and alternative method for the estimation of fatigue damage. ANN can provide accurate representations of the crack growth rate and cycle ratio from relatively small experiment data points. Also, ANN can predict fatigue damage behavior better than other current fatigue life estimation parameters. The following conclusions can, therefore, be drawn from the present review.

(1) The ANN optimized by initial learning conditions can learn crack growth rate da/dN within engineering error but can not generalize cycle ratio N/N_f within engineering error.

(2) Data transformation method which has good recognition quality improves learning and generalizing capacity of ANN much more than classical scaling method.

(3) ANN constructed by data transformation method has better generalization accuracy than learning accuracy.

(4) The estimation error of cycle ratio N/N_f with single parameter can be reduced by constructing ANN with various nondestructive and mechanical parameters.

References

Coffin, L. F., Jr., 1954, "A Study of the effects of Cyclic Thermal Stresses in a Ductile Metal," *ASME, Transactions*, Vol. 16, pp. 931~950.

Elber, W., 1970, The significance of Fatigue Crack Closure, Damage Tolerance in Aircraft Structures, STP-486, *ASTM*, pp. 230~243.

Hironobu Nisitani and Masahir Goto, 1985, "Relation between Small-crack Growth Law and Fatigue Life of Machines," *Journal of JSME*, Vol. 51, No. 462, pp. 332~341.

Hiroshi OKUDA, Hiroshi MIYZAKI, Genki YAGAWA, 1996, "Model of Inelastic Response using Neural Networks," *Int. J. of JSME (A)*, Vol. 62, No. 597, pp. 1284~1291.

Jang, D. Y., Cho, S. S. and Kim, D. J., 1999, "A Study on Fractal Property of Surface Microcrack Under Plane Bending Load," *Journal of Samcheok Nationl University (Korea)*, Vol. 31, pp. 35~49.

Joo, W. S. and Cho, S. S., 1996a, "A Study on High Temperature Low Cycle Fatigue Crack Growth Modeling by Neural Networks," Journal of the Korean Society of Mechanical Engineering (A), Vol. 20, No. 9, pp. 2752~2759.

Joo, W. S., Oh, S. W., Cho, S. S. and Hue, C. W., 1994a, "A Study on Fatigue Crack Growth Behavior at a Creep Temperature Region in SUS 304 Stainless Steel," *Journal of the Korean Society of Mechanical Engineering*, Vol. 18, No. 3, pp. 548~554.

Joo, W. S., Park, S. Y., Kim, D. J. Cho, S. S. and Jang, D. Y., 1998a, "A Study on Relationship of between X-ray Half-value Breadth and Cycle ratio in Al 2024-T3 Alloy Using Average gradient method," *1998 Fall Conference Proceeding (II), KSPE*, pp. 881~886.

Kim, D. S., 1992, *Neural networks-Theory and Application*, HiTech publisher, Seoul, pp. 97~144.

Kim, M. C., 1998, "A Study on Integrated Fatigue Damage Modeling Using Back-propagation Neural Networks," M.S. Thesis, *Dong-A University (Korea)*, pp. 11~22.

Mandelbert, B. B., 1983, *The Fractal Geometry*

of Nature, Freeman, Sanfrancisco, pp. 25~29.

Paris, P. C. and Erdogan, F., 1963, "A Critical Analysis of Crack Propagation Laws," *Trans. ASME, Basic Eng.*, Vol. 85, p. 528.

Park, S. Y., Kim, D. J., Cho, S. S., Joo, W. S. and Hong, S. H. 1998, "A Study on Estimation of Fatigue Life in SPCC Steel using X-ray Half-value Breadth," *2003 Spring Conference Proceeding (II)*, *KSAE*, pp. 768~774.

Tanaka. K., Hishide, T. and Maekawa, O, 1982,

"Surface-crack Propagation in Plane Bending Fatigue of Smooth Specimen of Low-Carbon Steel," *Eng. Frac. Mech.*, Vol. 16, No. 2, p. 207.

Wöhler, A., 1860, Versuche über die Festigkeit der Eisenbahnwagen-Achsen, Zeitchrift für Bauwesen.

X-Wu, J. Ghabousi, 1993, "Modeling The Cyclic Behavior of Concrete Using Adaptive Neural Network," *Computational Mechanics*, Vol. 1, pp. 1319~1329.